

Myocardial Perfusion Imaging and Dynamic Analysis with Technetium-99m Tetrofosmin

Kenichi Nakajima, Junichi Taki, Noriyuki Shuke, Hisashi Bunko, Shigeo Takata and Kinichi Hisada

Department of Nuclear Medicine and First Department of Internal Medicine, Kanazawa University Hospital, Kanazawa, Japan

Technetium-99m tetrofosmin is a new myocardial perfusion imaging agent that accumulates rapidly and shows slow clearance from the myocardium. Dynamic acquisition and SPECT imaging were performed in a total of 26 patients. Using exercise-rest protocol, the single-photon emission computed tomography (SPECT) findings of 130 myocardial segments were classified as infarction, ischemia and partial filling and compared to those with ^{201}Tl . Complete concordance of findings was obtained in 108 segments (83%) between images with $^{99\text{m}}\text{Tc}$ tetrofosmin and ^{201}Tl . Partial filling was observed in 24 segments with ^{201}Tl and 14 segments with tetrofosmin, showing a greater number of ischemic regions in ^{201}Tl . However, in comparison with coronary arteriography ($n = 19$), overall sensitivity and specificity for detecting coronary artery stenosis ($\geq 75\%$) was 15 of 25 (0.60) and 27 of 32 (0.84), respectively, which did not differ significantly from those of ^{201}Tl , which was 18 of 25 (0.72) and 27 of 32 (0.84), respectively. Graphic analysis that assumes unidirectional transfer of the tracer was applied to initial dynamic changes and uptake constant k and distribution volume V were computed. Multiple vessel disease and congestive heart failure showed a low perfusion index (k/V), and may be used in this type of tracer with unidirectional uptake. This preliminary study in the clinical trial showed the usefulness of $^{99\text{m}}\text{Tc}$ tetrofosmin as a myocardial perfusion imaging agent.

J Nucl Med 1993; 34:1478-1484

Current developments of $^{99\text{m}}\text{Tc}$ perfusion imaging agents demonstrate its usefulness in the diagnosis and management of ischemic heart disease (1,2). Two types of radiopharmaceuticals have been mainly used. The first type shows good accumulation in the myocardium with a long effective half-life (1-5). Technetium-99m sestamibi is a typical tracer of the retention-type. The second type of tracer shows rapid and high accumulation in the myocardium and clears rapidly, with $^{99\text{m}}\text{Tc}$ teboroxime a typical example (6-10). Technetium-99m tetrofosmin has a chemical form of 1,2-bis[bis(2-ethoxyethyl)phosphino] ethane and is considered to belong to the first type (11,12). Al-

though fundamental data in the kinetics and mechanism of uptake are still unsatisfactory, $^{99\text{m}}\text{Tc}$ tetrofosmin has been applied to clinical trials as a potentially useful myocardial imaging agent (11-18). In the present study, we investigated: (1) serial uptake of tetrofosmin in organs; (2) segmental comparison of findings between $^{99\text{m}}\text{Tc}$ tetrofosmin and ^{201}Tl SPECT; and (3) utility of perfusion index using graphical evaluation in which unidirectional transfer is assumed (19,20).

MATERIALS AND METHODS

Radiopharmaceutical Preparation

Technetium-99m tetrofosmin was supplied in kit form (Amersham Medical, Ltd., Japan). A vial contained 0.2 mg of 1,2-bis[bis(2-ethoxyethyl)phosphino] ethane. Technetium-99m pertechnetate (800-2200 MBq, 1-4 ml) was added to the vial and used after 10 min. From 260 to 740 MBq of $^{99\text{m}}\text{Tc}$ tetrofosmin was administered per study. Maximum patient dose was 1110 MBq. No adverse reaction was observed.

Subjects

Twenty-six patients were given both $^{99\text{m}}\text{Tc}$ tetrofosmin and ^{201}Tl in 1 wk. Six of the 26 had old myocardial infarction, five had angina pectoris, three had old myocardial infarction associated with angina, four had vasospastic angina, three had valvular heart disease, one had arrhythmogenic right ventricular dysplasia, one had hypereosinophilic syndrome, one had congestive heart failure and two were suspected of having ischemic heart disease associated with hypertension and diabetes mellitus. Coronary arteriography was performed on 19 patients. With $\geq 75\%$ stenosis considered to represent significant stenosis, three patients had triple-vessel disease, six had double-vessel disease, four had single-vessel disease and six had no significant stenosis, including one patient in whom coronary spasm was induced by ergometrine.

Exercise Protocol

Using a bicycle ergometer, multi-stage exercise was initiated from 25 W and increased by 25 W every 2 min. Exercise was continued until fatigue, chest discomfort and/or significant electrocardiographic changes suggesting ischemia occurred. A one-day protocol with exercise-rest sequence was used; a second resting study was repeated 3-4 hr later. The first administered dose of $^{99\text{m}}\text{Tc}$ tetrofosmin was 260-555 MBq; the second dose doubled the amount of the first.

In the ^{201}Tl study, 111 MBq of ^{201}Tl was injected intravenously at peak exercise. The multi-stage exercise procedure used in the tetrofosmin study also was applied. Delayed SPECT imaging was

Received Dec. 14, 1992; revision accepted May 25, 1993.

For correspondence or reprints contact: Kenichi Nakajima, MD, Dept. of Nuclear Medicine, Kanazawa University Hospital, 13-1 Takara-machi, Kanazawa, 920 Japan.

performed 3 hr later. The exercise endpoint did not differ significantly between the two studies.

Imaging Equipment

In planar and dynamic acquisition of ^{99m}Tc tetrofosmin, a large rectangular field camera-computer system (GCA/E2, GMS550U, Toshiba, Tokyo) was used. For ^{99m}Tc tetrofosmin SPECT, a triple-headed SPECT (GCA 9300A, GMS 550U, Toshiba, Tokyo) was used. For the ^{201}Tl SPECT study, either the triple-headed system or a dual-headed system (ZLC 7500, Scintipac 2400S, Shimadzu, Kyoto) was used.

Data Acquisition

Two types of dynamic acquisition were performed. In the first five patients dynamic acquisition was performed in anterior projection at rest. A series of 128×128 -matrix images was obtained with 30 sec per frame for 15 min. In 19 patients, 100 frames of 64×64 -matrix images were obtained by 1 sec per frame in the anterior chest view. In the second study of ^{99m}Tc tetrofosmin, background activity caused by the previous study was subtracted.

In the SPECT acquisition, 60 projection images were obtained with 128×128 matrix and 30 sec per view. A 360-degree acquisition method was employed by both triple-headed and dual-headed SPECT systems. Background activity from the first SPECT study was not corrected in the second. In addition, three 256×256 -matrix planar images were obtained in the anterior, left anterior oblique 42-degree and 72-degree projections. Although 64×64 -matrix projection images were used in the dual-headed system, the acquisition protocol was the same as in the triple-headed SPECT. In six initial patients, SPECT acquisition was repeated twice, approximately 0.5–1 hr and 3 hr after injection, to evaluate changes in accumulation pattern. In the next 20 patients, data acquisition was performed once, approximately 10 min to 1 hr after injection.

SPECT Image Reconstruction

After preprocessing projection images by a Butterworth filter with eighth order and cutoff frequency of 0.47 cycle/cm, transaxial images were reconstructed with filtered backprojection by a Ramp filter. Short-axis and vertical long-axis images were generated. Neither attenuation correction nor scatter correction was performed. The reconstruction procedure was identical for both dual-headed and triple-headed SPECT.

Dynamic Study Processing

In the first five patients in the planar study, regions of interests (ROIs) were drawn over the myocardium, right lung and liver. The hepatic ROI was set on the hepatic parenchyma, excluding the biliary tree. A time-activity curve was generated on each ROI.

Myocardial Perfusion Index by Graphical Analysis

In 19 patients, a perfusion index corresponding to the uptake constant was calculated. The graphical evaluation proposed by Patlak et al. was applied to the analysis of initial accumulation (19,20). In this analysis, no invasive method was attempted, although serial arterial concentration and tissue concentration were required. A ROI was set over the ascending aorta or arch in the anterior view (Fig. 1). Myocardial concentration was measured using a ROI over the left ventricular myocardium including the chamber cavity. Aortic activity was substituted to plasma, while heart activity corresponded to myocardial and blood-pool activity. No attenuation correction for the depth of aorta and heart was performed; timing of arrival to the aorta and myocardium was assumed to be the same. Assuming unidirectional transfer in a

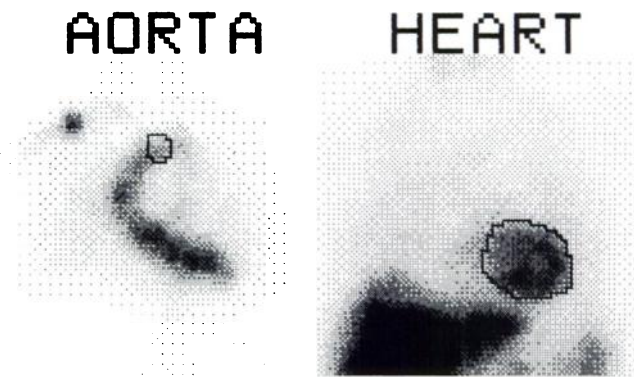


FIGURE 1. An example of ROI selection for initial dynamic analysis. Aortic ROI was set on the aortic arch using a composite image of arterial phase (left panel). Heart ROI was selected on the left ventricular myocardium using a later composite image (right panel). In this case, cutoff value for drawing ROI was 60% of maximum activity in each ROI.

certain period immediately after injection, the ratio of entire myocardial activity (A_{heart}) and aortic activity (C_a) was expressed as:

$$A_{\text{heart}}/C_a = k \left(\int_0^t C_a d\tau \right) / C_a + V,$$

where k is an uptake constant and V is the myocardial distribution volume plus blood volume (18). When this normalized integral time $[(\int_0^t C_a d\tau)/C_a]$ was plotted in the abscissa and heart-to-aortic activity ratio in the ordinate, a linear portion was always found. By using the least-square linear fitting method, the slope k and intercept V were determined. To eliminate effect of ROI size, we computed the ratio of k -to- V that was defined as the myocardial perfusion index, although not strictly an influx constant in an absolute sense.

The graphic analysis was technically validated before clinical application. The size and location of ROIs for calculating the ratio k -to- V were examined (Fig. 1). When an aortic ROI was set on the ascending portion near the aortic valve, its overlap on the pulmonary artery or right heart could not be avoided. We decided to set the aortic ROI on the aortic arch or the upper part of the ascending aorta, using the composite image of the aortic phase. A heart ROI was drawn on the summed image at 2–3 min when the myocardium was clearly visualized. The effect of ROI size on the parameter k/V was studied by setting various ROIs. Initially, larger polygonal or rectangular ROIs were placed on the aortic arch and heart. The various ROI sizes that were determined by the thresholding technique were used to calculate the index. Using all patients, the reproducibility of the fitting was examined by two operators independently and intraobserver variability was examined by an operator one month later. Because both k and V were equally affected by aortic ROI size, the ratio of k -to- V was employed as a perfusion index. By taking the ratios, the effect of ROI size was cancelled, since both numerator and denominator have aortic ROI size as their unit of volume.

SPECT Image Interpretation

Tomographic myocardial images were divided into five regions. Four segments of anterior, septal, inferoposterior and lateral walls were evaluated in the two slices of basal and apical short-axis cut. The apical segment was evaluated using a mid-portion of the

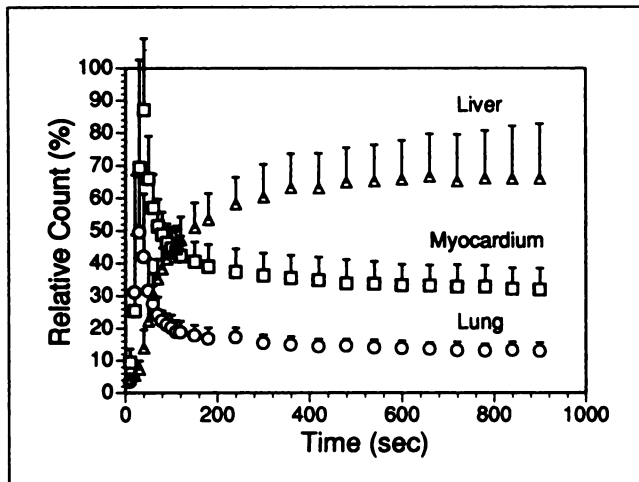


FIGURE 2. Time-activity curves by planar study on the heart, lung and liver. Mean and s.d. are shown ($n = 5$).

vertical long-axis section. Both ^{201}Tl and $^{99\text{m}}\text{Tc}$ tetrofosmin data were interpreted by blinded qualitative analysis. All SPECT images were analyzed by two nuclear medicine specialists with no prior knowledge of the patient's clinical information. Disagreement of interpretation was resolved by consensus. Myocardial accumulation was divided into five grades: normal, slightly reduced, moderately reduced, severely reduced and defect. When the degree of accumulation changed by one grade or more, it was considered a positive change. By comparing exercise and rest studies, findings were classified as normal, ischemia (complete filling), infarction (no filling), partial filling, heterogeneous perfusion and reverse filling. In ^{201}Tl findings, the term of redistribution can be used instead of filling.

Correlation between coronary artery stenosis and the SPECT

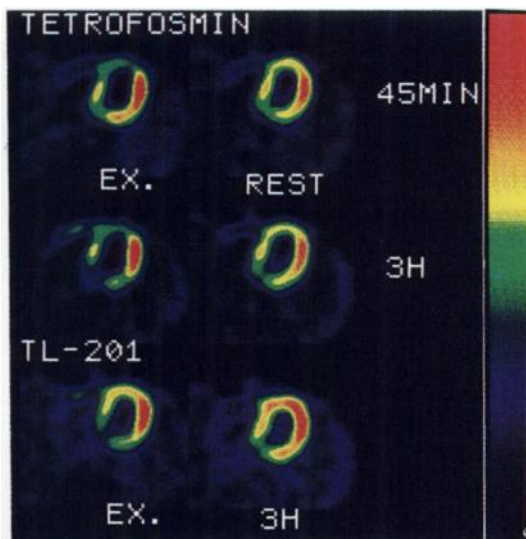


FIGURE 3. Technetium-99m tetrofosmin (upper and middle panels) and ^{201}Tl (lower panel) transaxial images in a patient with anteroseptal infarction. Background was not subtracted in each image. By coronary arteriography, 90% stenosis was observed in the left anterior descending and right coronary arteries. Technetium-99m tetrofosmin images from 45 min and 3 hr show no significant difference. Although both $^{99\text{m}}\text{Tc}$ tetrofosmin and ^{201}Tl show anteroseptal partial filling, the degree of decreased activity was more evident in the $^{99\text{m}}\text{Tc}$ tetrofosmin images.

TABLE 1
Time Course of Technetium-99m Tetrofosmin*

Time	Heart-to-lung ratio	Heart-to-liver ratio
5	2.36 ± 0.72	0.49 ± 0.05
10	2.49 ± 0.85	0.41 ± 0.08
15	2.67 ± 1.11	0.41 ± 0.12
45 [†]	2.74 ± 0.33	1.14 ± 0.51
180 [†]	2.80 ± 0.43	2.33 ± 0.54

* $n = 5$, mean and s.d.

[†]Measured with a static image after the first study.

data was studied in 19 patients who underwent coronary arteriography. The angiographic finding was considered positive when the stenosis was $\geq 75\%$, whereas myocardial SPECT finding was considered positive when infarction and/or ischemia were seen in the corresponding myocardial segments. In this comparison, we assumed that the left anterior descending artery (LAD) territory corresponded to the anterior, septal and apical segments; the right coronary artery (RCA) territory corresponded to the inferoposterior segments; and the left circumflex artery (LCX) territory corresponded to the lateral segment.

Statistics

Results were expressed as mean \pm s.d. The statistical difference in mean values between groups was analyzed using the Student's t-test. The difference of detectability for coronary artery stenosis was analyzed by chi-square test.

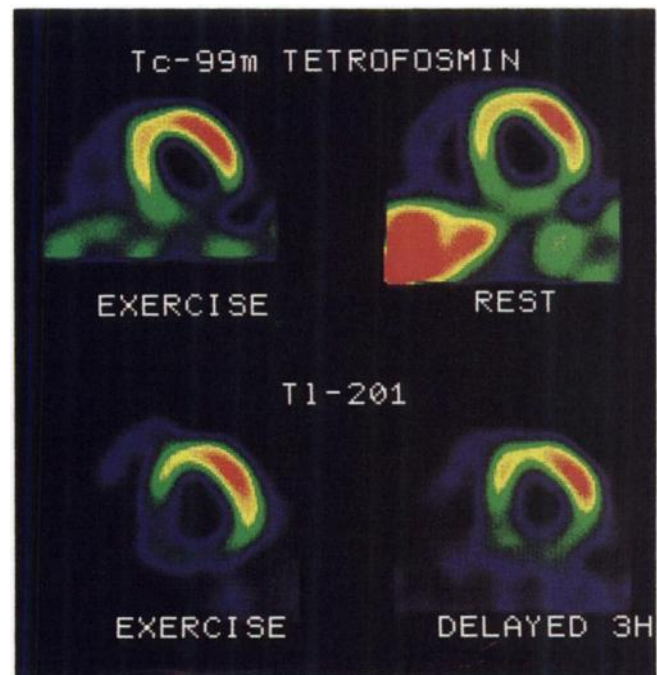


FIGURE 4. Technetium-99m tetrofosmin (upper panel) and ^{201}Tl (lower panel) short-axis images in a patient with inferoposterior infarction. Coronary arteriogram revealed 99% stenosis in the right coronary artery. Both tracers show decreased concentration in the inferior wall. However, ^{201}Tl demonstrated a larger hypoperfusion area than the $^{99\text{m}}\text{Tc}$ tetrofosmin studies. Slight filling of the inferior wall was observed in both studies.

TABLE 2
Comparison of Thallium-201 and Technetium-99m
Tetrofosmin Findings

Tetrofosmin	²⁰¹ Tl		Partial		Reverse		Total
	Normal	Ischemia	Infarct	filling	Uneven	filling	
Normal	65	2	0	6	2	0	75
Ischemia	0	0	1	0	0	0	1
Infarct	0	0	16	5	0	0	21
Partial filling	2	0	1	11	0	0	14
Uneven	0	0	0	1	16	0	17
Reverse filling	1	0	0	1	0	0	2
Total	68	2	18	24	18	0	130

Complete agreement = 108/130 segments (83%)

RESULTS

Serial Changes in the Dynamic Studies

In serial planar images, tetrofosmin activity in the myocardium reached a peak approximately 5 min later, and plateaued thereafter. An early time course for 15 min after intravenous injection is shown in Figure 2. Although initial myocardial activity rises quickly and decreases rapidly, it is due to overlap of left ventricular blood activity. Serial myocardium-to-lung ratio and myocardium-to-liver ratio determined by planar dynamic studies are shown in Table 1. Myocardium-to-lung ratio was high even after 5 min and gradually increased with time, reaching more than 2.5 after 15 min. Myocardium-to-liver ratio was about 0.4–0.5 in the initial 15 min and increased with time. Hepatic activity significantly decreased after 45 min.

SPECT Study

In 30 segments of the initial six studies, 0.5–1-hr images and 3-hr images were compared. No significant difference was observed on scan interpretation (Fig. 3). Table 2 shows a comparison between the ^{99m}Tc tetrofosmin and ²⁰¹Tl studies. Complete agreement was obtained in 108 segments (83%). Infarction was found in 21 segments with tetrofosmin and 18 segments with ²⁰¹Tl. Partial filling, which is considered to be ischemia plus infarction, was observed in 14 segments with tetrofosmin. Partial redistribution was seen in 24 segments with ²⁰¹Tl, demonstrating more ischemic segments in the ²⁰¹Tl study ($p < 0.01$). Heterogeneous segments were observed in hypereosinophilic syndrome with heart failure, arrhythmogenic right ventricular dysplasia, congestive heart failure and a part of vasospastic angina, and were in agreement in both studies.

The comparison between SPECT abnormality and significant coronary stenosis is summarized in Table 3 ($n = 19$). Sensitivity and specificity of ^{99m}Tc tetrofosmin to detect coronary artery stenosis was 15 of 25 (0.60) and 27 of 32 (0.84), respectively. The ²⁰¹Tl study showed sensitivity of 18 of 25 (0.72) and specificity of 27 of 32 (0.84). Overall diagnostic accuracy of ^{99m}Tc tetrofosmin was 42 of 57 (0.74) and that of ²⁰¹Tl was 45 of 57 (0.79). No significant statistical difference was observed between two studies regarding the detectability of coronary artery stenosis. In

TABLE 3
Comparison of Tetrofosmin and Thallium-201 Findings with
Coronary Arteriography

	Sensitivity		Specificity		Accuracy	
Tetrofosmin						
RCA	4/7		8/12			
LAD	7/9		9/10			
LCX	4/9		10/10			
Total	15/25	0.60	27/32	0.84	42/57	0.74
Thallium						
RCA	5/7		7/12			
LAD	9/9		10/10			
LCX	4/9		10/10			
Total	18/25	0.72	27/32	0.84	45/57	0.79

the ^{99m}Tc tetrofosmin study, nine coronary territories of partial filling were detected and six had significant stenosis. In the ²⁰¹Tl study, 12 territories of incomplete redistribution were observed and 10 had significant stenosis (n.s. versus ^{99m}Tc tetrofosmin study). A false-positive ischemic finding of the ²⁰¹Tl study was seen in two RCA territories and a LAD territory, while a false-positive finding of the tetrofosmin study was found in two RCA territories.

Typical findings of infarction and ischemia are shown in Figures 3 and 4.

Myocardial Perfusion Index

An example of the effect of ROI variation is shown in Table 4. In this case the aortic ROI was changed from a 40% cutoff (27 pixels) to a 60% cutoff (14 pixels). The heart ROI was similarly changed from a 40% cutoff (133 pixels) to a 60% cutoff (103 pixels). The variability of perfusion index was relatively small as shown in nine combinations. The average perfusion index was 2.48 ± 0.17 and the coefficient of variation (s.d./average) index was 7% (maximum 10%). Interobserver variability of the parameter k/V was $R = 0.85$ ($p < 0.001$), and intraobserver variability was $R = 0.86$ ($p < 0.001$).

An example of a result of graphic analysis and the linear fitting is shown in Figure 5. The average perfusion index in patients with no significant coronary artery stenosis ($n = 5$) was 2.00 ± 0.41 (s.d.), and arrhythmogenic right ventricular dysplasia showed the lowest perfusion index (0.21), although no coronary artery stenosis was seen. Single-vessel disease ($n = 3$) showed 2.22 ± 0.38 , whereas multiple-vessel disease ($n = 4$) showed 1.05 ± 0.61 . Although the number of subjects in each group was small, a statistically significant difference was calculated between normal and multiple-vessel diseases ($p = 0.026$) and between single-vessel and multiple-vessel disease ($p = 0.034$) by two-tailed unpaired t-test. A patient with hypereosinophilic syndrome, who had severe congestive heart failure and died 45 days later, also showed low perfusion index (0.62).

DISCUSSION

Technetium-99m Tetrofosmin Characteristics

Thallium-201 myocardial scintigraphy has become an indispensable diagnostic tool in the evaluation of myocar-

TABLE 4
Effect of ROI Variation on the Perfusion Index k/V

	Cutoff (%)	Pixel	ROI size of the aorta			Average	s.d.	c.v.
			60% 14	50% 19	40% 27			
ROI size of the heart	60%	103	2.40	2.46	2.40	2.42	0.03	0.01
	50%	120	2.32	2.52	2.72	2.52	0.20	0.08
	40%	133	2.40	2.33	2.80	2.51	0.25	0.10
	average		2.38	2.43	2.64	2.48*		
	s.d.		0.05	0.09	0.21		0.17*	
	c.v.		0.02	0.04	0.08			0.07*

*Statistics in nine combinations. s.d. = standard deviation, c.v. = coefficient of variation.

dial perfusion. The unique characteristics of ^{201}Tl , such as high uptake in myocardium and the redistribution phenomenon, have been applied to various cardiac diseases, including ischemic heart disease, cardiomyopathy and valvular heart disease. Currently, however, $^{99\text{m}}\text{Tc}$ -labeled imaging agents have been added to myocardial perfusion studies (1,2). Two types of $^{99\text{m}}\text{Tc}$ agents typified by $^{99\text{m}}\text{Tc}$ teboroxime and $^{99\text{m}}\text{Tc}$ sestamibi are clinically available. Since $^{99\text{m}}\text{Tc}$ teboroxime accumulates rapidly and significantly in the myocardium in a few minutes and clears away quickly, special care is required to obtain good quality SPECT images (1,8,10). On the other hand, sestamibi is a retention-type radiopharmaceutical and is more suitable for SPECT acquisition. Technetium-99m tetrofosmin is a retention-type agent and shows no redistribution (11-13). Although the second and third clinical trials have been completed, the fundamental characteristics and mechanism of accumulation have not yet been clarified. Recent studies on $^{99\text{m}}\text{Tc}$ tetrofosmin have shown high myocardial activity and relatively rapid liver clearance, providing a

favorable biokinetic profile for myocardial imaging (14-18). In addition, preliminary clinical studies have shown adequate sensitivity and specificity to assess patients with coronary artery disease. This study demonstrates a good quality myocardial perfusion image as soon as 10 min after intravenous injection, which was in early dynamic studies. After 15 min, the myocardium-to-lung ratio was more than 2.5 and the myocardium-to-liver ratio was more than 0.4, including patients with various cardiac diseases. In a recent study of $^{99\text{m}}\text{Tc}$ tetrofosmin, Higley et al. report higher heart-to-lung ratio (3.1 ± 1.8 at 5 min and 7.3 ± 4.4 at 60 min) in normal volunteers (29).

Regarding liver clearance, although hepatic accumulation was initially observed, it did not significantly interfere with the inferior myocardial wall by Compton scatter. SPECT data acquisitions after 45 min are preferable since hepatic activity was reduced more than myocardial activity. However, SPECT acquisition after 15 min is feasible and can provide a good quality image.

In a $^{99\text{m}}\text{Tc}$ -sestamibi study, Wackers et al. report that heart-to-lung ratios at 5-min, 60-min and 180-min rest images were 1.9 ± 0.2 , 2.4 ± 0.1 and 2.7 ± 0.2 , respectively, at rest, and heart-to-liver ratios were 0.5 ± 0.1 , 0.6 ± 0.1 and 1.4 ± 0.2 , respectively (3). In our $^{99\text{m}}\text{Tc}$ tetrofosmin study, the heart seemed to accumulate relatively higher activity and the liver showed relatively lower activity than in Wackers' $^{99\text{m}}\text{Tc}$ -sestamibi study, particularly 1 hr after injection. A minimum dose of 260 MBq (~ 7 mCi) provided sufficiently good perfusion images for the first study. The myocardial uptake pattern did not change for at least 3-4 hr. Since heating to 100°C is not necessary as with $^{99\text{m}}\text{Tc}$ sestamibi, tetrofosmin can be a convenient imaging agent for rapid preparation.

Agreement with the Thallium-201 Study and Coronary Arteriography

In comparison with coronary arteriography, the detectability of significant coronary artery stenosis ($\geq 75\%$) was slightly lower in the $^{99\text{m}}\text{Tc}$ tetrofosmin study, but the difference was not statistically significant.

Although data are limited in study of 26 patients, complete agreement of the SPECT findings was obtained in 83% (108/130) between the two radiopharmaceuticals. This

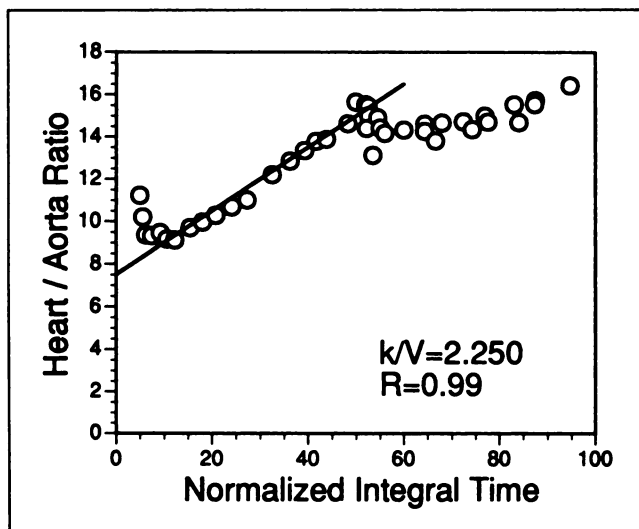


FIGURE 5. Graphic evaluation of $^{99\text{m}}\text{Tc}$ tetrofosmin dynamic curve. When points of heart-to-aortic ratio (A_{heart}/C_a) versus normalized integral time ($(\int_0^t C_a d\tau)/C_a$) are plotted, linear portions are found. A fitted line by the least-square method is drawn in the graph. The intercept V corresponds to the volume of tracer distribution.

agreement was similar to that seen in ^{99m}Tc -sestamibi and ^{99m}Tc -teboroxime studies (1). Technetium-99m tetrofosmin showed lower detectability of ischemia associated with infarction (partial filling). Since our ^{201}Tl study protocol did not use a reinjection protocol (25–27), one would suspect a greater degree of underestimation of ischemia in the ^{99m}Tc tetrofosmin study. The extraction fraction of tetrofosmin might be lower than that of ^{201}Tl , although this has not yet been clarified. Sinusas et al. reported that myocardial tetrofosmin activity exceeded microsphere flow in low flow (<30% of nonischemic) regions, while tetrofosmin activity was less than microsphere flow in high flow (>130% of nonischemic) regions (18). Real difference could thus exist at high-flow range, which may be observed at exercise or at the lower flow range as in ischemia.

Physical property caused by the difference of ^{99m}Tc and ^{201}Tl may be involved. However, since the difference was seen in any coronary artery territories, it is probably related to the pharmacological or physiological difference of the two tracers, rather than the difference of the physical properties of ^{201}Tl and ^{99m}Tc , such as the attenuation of the inferoposterior wall.

Another factor is overlap of the second tracer activity on initial distribution. A difference in protocol may alter detectability such as the same-day protocol with rest-exercise or exercise-rest sequence or a two-day protocol. This finding should be more carefully examined by increasing the number of patients. Overall, however, the high agreement rate (83%) in this preliminary study encourages further study of ^{99m}Tc tetrofosmin.

Possible Utility of Perfusion Index by a Graphic Evaluation

Patlak (19,20) proposed graphic evaluation in tracers with unidirectional transfer, which has been applied to analysis of glucose metabolism and receptor studies (19–21) and in other organs (22–24,28). Neither a specific compartmental model nor a numerical solution of the parameter is necessary. Uptake constant can be computed using a simple linear fitting. If the ratio of the arterial plasma concentration-time integral-to-plasma concentration is plotted in the abscissa and a ratio of tissue and plasma concentration is plotted in the ordinate, the uptake constant can be estimated by the slope of the linear portion with the intercept of the fitted line nearly corresponding to the vascular plus steady state space (18). The constant presence of linear portion in the tetrofosmin study indicates that unidirectional transfer can be assumed at least in the initial phase. However, our approach did not measure true tissue concentration or plasma concentration. Our objective was to describe a more simple and practical method of perfusion index and to compare results with clinical information, rather than to achieve complete quantitative modeling.

The ROI size also influences results. In aortic ROI as an input function both k and V were equally influenced by aortic ROI size. Since we employed the index of the ratio k -to- V , which is not influenced by ROI size of input func-

tion, variability was generally small, as shown by the average of coefficient variation = 7%. In our experience, variation of heart ROI was generally small, since the left ventricular myocardium was clearly visible in the later images. Overall reproducibility of the parameter was considered acceptable. However, if the aortic ROI is not clearly visible because of congenital heart disease and technically poor bolus injection or other factors, we should interpret the results carefully.

The difference of tracer arrival time between the myocardium and the aortic arch was not corrected. Generally in nuclear medicine analysis, the input function has been set on the ROI near the target organ or heart, which expresses the arterial time activity changes. However, in myocardial imaging agents, an aortic ROI would be preferred in order to exclude myocardial activity. Since it was difficult to measure the difference in arrival time of activity between the myocardium and the aortic arch, particularly in planar studies, we assumed that arrival time was approximately the same.

Aortic activity was not calibrated by serial arterial sampling. However, a similar approach has been used in planar studies of other organs, such as the kidneys and the brain (22–24), and useful indices have been reported (28). Considering the noninvasive approach and our goal to make a practical index of perfusion, we accepted this aortic activity as a substitute for input function. The influence of lung activity to the heart was also not corrected, because during the first transit of the tracer each organ was relatively well separated anatomically and temporally in the anterior view.

At present, quantification by SPECT has several problems, including Compton scatter correction, attenuation correction and the need for more rapid dynamic SPECT acquisition. We used k/V to determine its suitability as an index of perfusion or if it correlated with pathophysiology. When the quantitative aspects of SPECT are improved, this parameter will have more physiological meaning as the uptake constant in an absolute sense. It is interesting to note, however, that patients with multiple-vessel disease and congestive heart failure show significantly lower values. This graphic approach required only planar dynamic acquisition, and data processing is simple and rapid for a computer. It may also be applied to other radiopharmaceuticals that are assumed to show unidirectional uptake for a certain period after injection.

CONCLUSION

A preliminary study with ^{99m}Tc tetrofosmin showed good agreement with ^{201}Tl SPECT findings and may be a promising radiopharmaceutical for myocardial perfusion imaging. A difference in detectability of ischemia was noted. However, compared with coronary arteriography, the diagnostic accuracy to detect coronary stenosis in the ^{99m}Tc tetrofosmin study did not differ significantly from those of the ^{201}Tl study. The myocardial perfusion index by

graphic analysis seems to reflect the severity of coronary artery disease and congestive heart failure.

ACKNOWLEDGMENT

This work was carried out as a part of Phase 2 and 3 clinical trials of ^{99m}Tc tetrofosmin (Amersham Medical Ltd., Tokyo).

REFERENCES

1. Leppo JA, DePuey EG, Johnson LL. A review of cardiac imaging with sestamibi and tetrofosmin. *J Nucl Med* 1991;32:2012-2020.
2. Beller GA, Watson DD. Physiological basis of myocardial perfusion imaging with the technetium-99m agents. *Semin Nucl Med* 1991;21:173-181.
3. Wackers FJ, Berman DS, Maddahi J, et al. Technetium-99m hexakis 2-methoxyisobutyl isonitrile: human biodistribution, dosimetry, safety and preliminary comparison to thallium-201 for myocardial perfusion imaging. *J Nucl Med* 1989;30:301-311.
4. Gibbons RJ. Technetium-99m sestamibi in the assessment of acute myocardial infarction. *Semin Nucl Med* 1991;21:213-222.
5. Kahn JK, McGhie I, Akers MS, et al. Quantitative rotational tomography with ²⁰¹Tl and ^{99m}Tc 2-methoxy-isobutyl-isonitrile. A direct comparison in normal individuals and patients with coronary artery disease. *Circulation* 1989;79:1282-1293.
6. Narra RK, Nunn AD, Kuczynski BL, Feld T, Wedeking P, Eckelman WC. A neutral technetium-99m complex for myocardial imaging. *J Nucl Med* 1989;30:1830-1837.
7. Seldin DW, Johnson LL, Blood DK, et al. Myocardial perfusion imaging with technetium-99m SQ30,217: comparison with thallium-201 and coronary anatomy. *J Nucl Med* 1989;30:312-319.
8. Stewart RE, Schwaiger M, Hutchins GD, et al. Myocardial clearance kinetics of technetium-99m-SQ30217: a marker of regional myocardial blood flow. *J Nucl Med* 1990;31:1183-1190.
9. Dahlberg ST, Weinstein H, Hendel RC, McSherry B, Leppo JA. Planar myocardial perfusion imaging with Tc-99m-tetrofosmin: comparison by vascular territory with thallium-201 and coronary angiography. *J Nucl Med* 1992;33:1783-1788.
10. Nakajima K, Taki J, Bunko H, et al. Dynamic acquisition with a three-headed SPECT system: application to technetium-99m-SQ30217 myocardial imaging. *J Nucl Med* 1991;32:1273-1277.
11. Kelly JD, Higley B, Archer CM, et al. New functional diphosphine complex of Tc-99m for myocardial perfusion imaging [Abstract]. *J Nucl Med* 1989;30:773.
12. Smith FW, Smith T, Gemmell HG, et al. Phase I study of Tc-99m diphosphine (P53) for myocardial imaging [Abstract]. *J Nucl Med* 1991;32:967.
13. Lahiri A, Higley B, Crawley JCW, et al. Novel functionalized diphosphine complexes of Tc-99m for myocardial imaging in man [Abstract]. *J Nucl Med* 1989;30:818.
14. Jain D, Mattera JA, Sinusas A, et al. Biokinetics of Tc-99m-tetrofosmin, a new myocardial imaging agent: implications for one day imaging protocol [Abstract]. *J Nucl Med* 1992;33:874.
15. Leclercq B, Lalock MP, Braat S, Lahiri A, Itti R, Rigo P. Clinical efficacy of tetrofosmin, a new Tc-labeled myocardial imaging agent [Abstract]. *J Nucl Med* 1992;33:874.
16. Rigo P, Braat S, Itti R, et al. Myocardial imaging with technetium-99m P53, comparison with thallium in suspected coronary artery disease [Abstract]. *J Am Coll Cardiol* 1992;19:202.
17. Sridehara BS, Itti R, Braat S, et al. Technetium-99m-tetrofosmin—a new myocardial imaging agent for evaluation of coronary heart disease [Abstract]. *J Nucl Med* 1992;33:875.
18. Sinusas AJ, Shi OX, Saltzberg MT, et al. Technetium-99m tetrofosmin for assessment of myocardial perfusion: initial distribution and clearance, relationship to blood flow [Abstract]. *J Nucl Med* 1992;33:993.
19. Patlak CS, Blasberg RG, Fenstermacher JD. Graphical evaluation of blood-to-brain transfer constants from multiple-time uptake data. *J Cereb Blood Flow Metabol* 1983;3:1-7.
20. Patlak CS, Blasberg RG. Graphical evaluation of blood-to-brain transfer constants from multiple-time uptake data. Generalization. *J Cereb Blood Flow Metabol* 1985;5:584-590.
21. Wong DF, Gjedde A, Wagner HN Jr. Quantification of neuroreceptors in the living human brain. I. Irreversible binding of ligands. *J Cereb Blood Flow Metabol* 1986;6:137-146.
22. Rutland MD. A comprehensive analysis of renal DTPA studies. I. Theory and normal values. *Nucl Med Commun* 1985;6:11-20.
23. Takeshita G, Maeda H, Nakane K, et al. Quantitative measurement of regional cerebral blood flow using N-isopropyl-(iodine-123) p-iodoamphetamine and single-photon emission computed tomography. *J Nucl Med* 1992;33:1741-1749.
24. Matsuda H, Tsuji S, Shuke N, Sumiya H, Tonami N, Hisada K. A quantitative approach to technetium-99m hexamethylpropylene amine oxime. *Eur J Nucl Med* 1992;19:195-200.
25. Dilsizian V, Rocco TP, Freedman NMT, Leon MB, Bonow RO. Enhanced detection of ischemic but viable myocardium by the reinjection of thallium after stress-redistribution imaging. *N Engl J Med* 1990;323:141-146.
26. Rocco TP, Dilsizian V, McKusick KA, Fischman AJ, Boucher CA, Strauss HW. Comparison of thallium-201 redistribution with rest "reinjection" imaging for the detection of viable myocardium. *Am J Cardiol* 1990;66:158-163.
27. Tamaki N, Ohtani H, Yonekura Y, et al. Significance of fill-in after thallium-201 reinjection following delayed imaging: comparison with regional wall motion and angiographic findings. *J Nucl Med* 1990;31:1617-1623.
28. Peters AM. A unified approach to quantification by kinetic analysis in nuclear medicine. *J Nucl Med* 1993;34:706-713.
29. Higley B, Smith FW, Smith T, et al. Technetium-99m-1,2-bis[bis(2-ethoxyethyl)phosphino]ethane: human biodistribution, dosimetry and safety of a new myocardial perfusion imaging agent. *J Nucl Med* 1993;34:30-38.